Absolute Rate Constant of the OH + ClO Reaction at Temperatures between 218 and 298 K

Jin Jin Wang and Leon F. Keyser*

Atmospheric Chemistry Element, Earth and Space Sciences Division, Jet Propulsion Laboratory, California Institute of Technology, Pasadena, California 91109

Received: June 26, 2001; In Final Form: August 28, 2001

The total absolute rate constant ($k_{1a} + k_{1b}$) for the reactions OH + ClO → Cl + HO_2 (k_{1a}) → HCl + O_2 (k_{1b}) has been determined in the temperature range from 218 to 298 K at a total pressure of 1 Torr of helium. Pseudo-first-order conditions were used with ClO in large excess over initial OH. ClO was produced by reacting Cl atoms with an excess of O_3; both ClO and O_3 were quantitatively determined by UV spectrophotometry between 210 and 310 nm. Two sources of OH were used: the reaction of F atoms with excess water vapor and the reaction of H atoms with an excess of NO_2. OH was monitored by resonance fluorescence near 308 nm. The absolute rate constant was determined from plots of ln [OH] vs time and absolute ClO concentrations. At 298 K, the result is $(2.22 \pm 0.33) \times 10^{-11}$ cm^3 molecule^{-1} s^{-1}. The temperature dependence expressed in Arrhenius form is $(7.2 \pm 2.2) \times 10^{-12}$ exp[$(333 \pm 70)/T$] cm^3 molecule^{-1} s^{-1}. The uncertainties are at the 95% confidence limits and include statistical errors from the data analysis and estimates of systematic experimental errors. Numerical simulations show that under the experimental conditions used secondary reactions did not interfere with the measurements. Numerical simulations and experimental checks also show negligible loss of ClO between the time when it is determined by UV absorption and the start of the OH + ClO reaction.

Introduction

The reaction of OH with ClO (eq 1) is important in partitioning reactive and nonreactive forms of chlorine in the

$$OH + ClO \rightarrow Cl + HO_2 \quad (1a)$$

$$OH + ClO \rightarrow HCl + O_2 \quad (1b)$$

stratosphere. Reaction pathway 1a interconverts reactive species in the HO_x and ClO_x families and is a chain propagation step. Pathway 1b converts two radical species to relatively inert reservoir species and serves as a chain termination step. The effect of reaction 1 on stratospheric chlorine chemistry is very sensitive to the branching ratio of these two pathways and to the absolute rate constant for the total reaction.[1] We recently measured the HCl yield, $k_{1b}/(k_{1a} + k_{1b})$, and found a value of $(9.0 \pm 4.8)\%$.[2] In the present study, we determine the absolute total rate constant for this reaction.

Previous measurements of k_1 at 298 K range from 9.1×10^{-12} to 24.4×10^{-12} cm^3 molecule^{-1} s^{-1}.[3−9] ClO was produced by reacting Cl atoms with O_3, OClO, or Cl_2O:

$$Cl + O_3 \rightarrow ClO + O_2 \quad (2)$$

$$Cl + OClO \rightarrow 2\ ClO \quad (3)$$

$$Cl + Cl_2O \rightarrow ClO + Cl_2 \quad (4)$$

In the earliest studies,[3,4] absolute concentrations of ClO were determined by equating [ClO] to initial O_3 or Cl_2O; later studies have shown that stoichiometric conversion to ClO cannot be assumed.[7,9,10] Also, some of the early studies[3−5,7] used excess Cl atoms, which requires a correction for the regeneration of OH by reaction 5b.

$$Cl + HO_2 \rightarrow HCl + O_2 \quad (5a)$$

$$Cl + HO_2 \rightarrow OH + ClO \quad (5b)$$

These issues could explain some of the disagreement among the results. To avoid the correction for reaction 5b, several more recent studies[6−9] reacted Cl atoms with excess O_3 to form ClO. Three of the previous studies[6,8,9] reported a slight negative temperature dependence, and two studies[4,5] found the reaction to be temperature-independent.

In the present study, a discharge-flow system is used to determine the absolute rate constant of reaction 1 in the temperature range from 218 to 298 K. Pseudo-first-order conditions are used with [ClO] ≫ [OH]. The rate constant is determined directly from the slopes of ln [OH] vs time plots and absolute [ClO]. Numerical models are used to assess the importance of secondary chemistry. The results are compared with previous measurements of this rate constant.

Experimental Section

The apparatus used in the present study has been described in detail recently,[2,11] and only a brief summary is presented here.

Reactor. The temperature-controlled Pyrex main reactor has an internal diameter of 5.04 cm and is 62 cm in length. At the downstream end, it is connected to a stainless steel resonance fluorescence cell. Pressure is measured by using a 10 Torr capacitance manometer connected to a port between the reactor

* To whom correspondence should be addressed. Fax: (818) 354-5148. E-mail: Leon.F.Keyser@jpl.nasa.gov.

10.1021/jp012426l CCC: $20.00
Published on Web 10/25/2001

and the fluorescence cell. At the upstream end are connections to a fixed ClO source and a movable OH source described in separate sections below. The inner surface of the reactor and outer surface of the movable OH source are coated with halocarbon wax to minimize wall loss of reactive species. Temperatures in the reaction zone are maintained within ±2 K by using refrigerated bath circulators to pass heat-exchange fluids (water or methanol) through a cooling jacket. Temperatures are monitored by two thermocouples located inside each end of the cooling jacket. Upstream of the main reaction zone, the reactants pass through a precooling region the length of which depends on the position of the movable source; average lengths are about 50 cm, which gives residence times near 50 ms. This region allows the reactants to cool from room temperature to the main reactor temperature before the reaction starts.

ClO Source. ClO is formed by reacting Cl atoms with an excess of O_3 (eq 2) in a fixed 5.0 cm diameter reactor located upstream of the main reaction zone; all surfaces except the Cl_2 discharge region are coated with halocarbon wax. Cl atoms are produced in a 2.45 GHz discharge (50 W) of dilute mixtures of Cl_2 in He. Ozone is formed by passing O_2 through a high voltage discharge ozonator and trapping the O_3 on silica gel at 195 K; the excess O_2 is pumped off and the O_3 is added to the source by passing a stream of He through the cold silica gel trap. Conditions are set so that the Cl + O_3 reaction is complete before the ClO exits the reactor.

ClO and O_3 Determination. After formation in the source reactor, the ClO is passed through a quartz absorption cell 3.0 cm in diameter and 50.1 cm in length; the cell walls, windows, and all connecting tubes downstream are also coated with halocarbon wax. ClO and O_3 are quantitatively determined by using absorption spectrophotometry in the UV between 210 and 310 nm. The collimated output of a 30 W deuterium lamp passes through the absorption cell and is focused on the entrance slit of a 0.3 m imaging spectrograph. A 600 groove/mm grating is used with an entrance slit width of 20 μm to give a resolution of 0.26 nm (fwhm) as determined by using the Hg line at 253.65 nm. The absorption spectrum is recorded by using a photodiode array situated at the exit focal plane of the spectrograph. To avoid any saturation effects, the exposure time is set to 0.25 s, which is at the middle of the linear response region of the diodes under our experimental conditions. A low-pressure Hg lamp is used to calibrate the wavelength scale of the spectrograph−diode array detector by recording several atomic lines between 253.65 and 334.15 nm.

The observed spectrum is a sum of O_3 and ClO spectra; to separate them, a spectral subtraction method is used. This technique has been described in detail[2,9] and will not be discussed here. Both ClO and O_3 are determined at 253.65 nm by using eq 6, where M is ClO or O_3, A is the absorbance defined by eq 7, σ_M is the absorption cross section, and L is the absorption path length.

$$[M] = A/(\sigma_M L) \tag{6}$$

$$A = \ln[(I_o - I_b)/(I_t - I_b)] \tag{7}$$

In eq 7, I_o, I_b, and I_t are the incident, background, and transmitted light intensities, respectively. The cross sections used are 11.58×10^{-18} cm^2 molecule^{-1} for O_3[12] and 4.23×10^{-18} cm^2 molecule^{-1} for ClO.[13−17]

Generally the total flow rates, pressures, and temperatures in the absorption cell differ from those in the main reactor. Therefore, to determine ClO and O_3 concentrations in the main reactor, their concentrations measured in the absorption cell are adjusted by using eq 8

$$[M]_m = (P_m/P_a)(F_a/F_m)(T_a/T_m)[M]_a \tag{8}$$

where M is ClO or O_3, P is the total pressure, F is the total flow rate, and T is the absolute temperature; the subscripts m and a refer to the main reactor and the absorption cell, respectively. To minimize calibration errors, the same flow meter and pressure gauge are used for the measurements in the absorption cell and the main reactor. Production efficiencies based on the fraction of initial Cl_2 converted to ClO average between 60% and 75%.

OH Sources. At temperatures between 260 and 298 K, a movable injector is used to produce OH by adding F atoms to an excess of water vapor (eq 9). The F atoms are produced in

$$F + H_2O \rightarrow OH + HF \tag{9}$$

a 2.45 GHz discharge of dilute F_2 in helium. An alumina tube is used for the F_2 discharge, which is operated at a total power of about 20 W. All surfaces except the discharge tube are coated with halocarbon wax. Water vapor is added by passing a stream of helium through a water bubbler maintained at 18 °C. Flow rates of H_2O are determined from the He flow rate, the total pressure, and the vapor pressure of H_2O. Typically, H_2O concentrations in the source are about 2.8×10^{14} molecules cm^{-3}. The reaction length is set to give a reaction time near 2.5 ms. Using $k_9 = 1.4 \times 10^{-11}$ cm^3 molecule^{-1} s^{-1},[18] we calculate that reaction 9 is complete for all the experimental conditions used. On the basis of the initial concentrations of F_2 added, reaction efficiencies to form OH average 55%.

At 218 and 239 K, OH is generated by adding H atoms to an excess of NO_2 (eq 10). The H atoms are formed in a microwave

$$H + NO_2 \rightarrow OH + NO \tag{10}$$

discharge of dilute mixtures of H_2 in He; a quartz tube is used at powers near 20 W. Again, all surfaces except the discharge region are wax coated. In the source, concentrations of NO_2 and O_2 are each about 3×10^{13} molecules cm^{-3}. The reaction time is set at 3 ms. Using $k_{10} = 4.0 \times 10^{-10} \exp(-340/T)$ cm^3 molecule^{-1} s^{-1},[18] we estimate the reaction is complete before OH is added to ClO in the main reactor. On the basis of initial H_2 concentrations, reaction efficiencies to form OH by reaction 10 average about 70%.

OH Detection. Hydroxyl radicals are detected by resonance fluorescence at a fixed point downstream of the reaction zone. A resonance lamp operated at 50 W of microwave power is used to excite the OH fluorescence. A stream of He saturated with water vapor is passed through the lamp at a total pressure near 4.5 Torr. Hydroxyl radical fluorescence near 308 nm is detected at right angles to the lamp by using an interference filter, photomultiplier tube, amplifier-discriminator, and dual counter−timer interfaced to a computer for data acquisition and analysis. The filter is placed between the photomultiplier and a suprasil quartz window that makes the vacuum seal to the flow tube, so the filter is never in contact with any of the reagents used. A Corning filter (0-53) is placed in front of the OH lamp to cut off radiation at wavelengths shorter than about 290 nm.

OH Calibration. Although we do not need absolute concentrations of OH to determine the rate constant, we want to know them as well as possible to do accurate modeling of the reaction. The system is calibrated by generating specific amounts of OH by adding known concentrations of NO_2 to an excess of

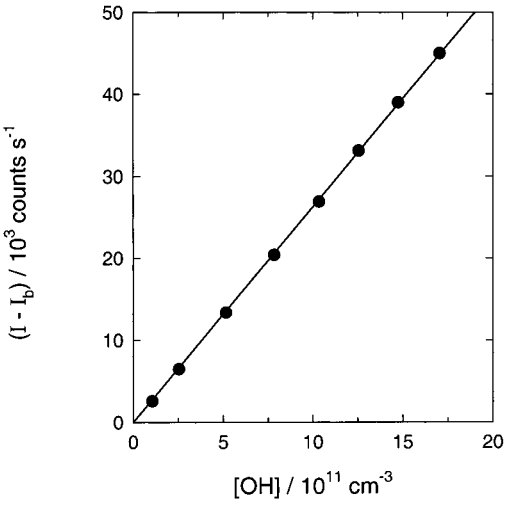

Figure 1. OH resonance fluorescence intensity vs [OH]. The response is linear over the range of [OH] used in this study; the line is a linear least-squares fit to the data.

H atoms (eq 10). H atoms are generated in a fixed microwave discharge (60 W) of dilute mixtures of H_2 in He. NO_2 in He mixtures of specific composition are prepared by using a calibrated capacitance manometer; the mixtures are stored in a 5 L Pyrex flask for later use. A calibrated flow meter is used to add known flows of the NO_2 in He mixture through the movable injector. Initial OH concentrations are corrected for wall loss and for self-reaction (eq 11) by using $k_{11} = 4.2 \times 10^{-12}$ $\exp(-240/T)$ cm^3 molecule^{-1} s^{-1}.[18]

$$OH + OH \rightarrow O + H_2O \qquad (11)$$

Typical OH fluorescence sensitivities are about 2.3×10^{-8} counts s^{-1}/(molecules cm^{-3}) with background signals of 1000 counts s^{-1}. For the 50 s counting times used, the minimum detectable [OH] is about 3×10^8 molecules cm^{-3} at a signal-to-noise ratio of unity. A plot of OH fluorescence intensity vs [OH] is shown in Figure 1. The signal is linear with respect to [OH] up to at least 2×10^{12} molecules cm^{-3}. This range covers the [OH] used in the present study.

Meter Calibrations. Mass flow meters and controllers are calibrated directly by using the volume change at constant pressure (bubble meter) method or by using the pressure rise at constant volume method. Pressure gauges are calibrated by using an oil manometer. All thermocouples used in the experiments are calibrated at 273 and near 195 K by using ice plus water and CO_2 plus methanol baths, respectively. Barometric corrections are used to obtain the CO_2 equilibrium temperature. The temperature in the reaction zone is measured by using a thermocouple probe in place of the movable inlet. At low temperatures, the probe reading is 1−2 K lower than the two thermocouples in the cooling jacket, while at 298 K, the probe temperature is within 0.2 K. All temperatures reported are based on the probe readings.

Reagents. Gases used are research grade He and H_2, each at 99.9999%, research grade Cl_2 (99.999%), ultrahigh purity O_2 (99.8%), 1% and 5% mixtures of F_2 in He, and CP grade NO (99% min). As described above (see ClO source), O_3 is formed by passing O_2 through a high-voltage discharge. NO_2 for OH calibrations is prepared from NO by adding an excess of O_2 and letting the mixture stand overnight. The excess O_2 is removed by pumping the mixture through a trap at 195 K, where the NO_2 condenses as a white solid; then mixtures in He are prepared by warming the solid and allowing the NO_2 gas to expand into a 5 L flask to which He is then added. NO_2 for use in the OH source is produced by adding an excess of O_2 to NO and storing the mixture in a thermally insulated Pyrex flask of known volume (4821 cm^3). The main carrier He is further purified by passage through a molecular sieve (Linde 3A) trap at 77 K just prior to use.

Results

Experimental Conditions. Concentrations of ClO are in the range of 2.8×10^{12} to 2.2×10^{13} cm^{-3} with initial OH concentrations from 2×10^{11} to 1×10^{12} cm^{-3}. Initial stoichiometric ratios range from 7 to 52 and average greater than 25. Concentrations of O_3 are between 6×10^{12} and 7×10^{13} cm^{-3}. Temperatures are in the range of 217.5 to 297.8 K at a total pressure of 1 Torr of helium. ClO is added to the system by turning on the Cl_2 flow to the fixed microwave discharge upstream of the ClO source reactor. ClO is removed by turning off the Cl_2 flow with all other flows held constant.

Data Analysis. Under these conditions, loss of OH is pseudo-first-order. When ClO is added to the system, the loss of OH may be written

$$d[OH]^+/dt = k_1[ClO][OH] + k_L^+[OH] \qquad (12)$$

Because the OH resonance fluorescence intensity, I_{OH}, varies linearly with [OH] (see Figure 1), we can write

$$k_I^+ \equiv -d\ln(I_{OH}^+)/dt = k_1[ClO] + k_L^+ \qquad (13)$$

where k_I^+ is the total pseudo-first-order rate constant for the loss of OH with added ClO. The parameter k_L^+ is the loss of OH other than by reaction with ClO; it includes wall loss, secondary reactions with species in the OH and ClO sources, and reactions with species formed by the OH + ClO reaction itself. In the absence of added ClO, we may write

$$k_I^- \equiv -d\ln(I_{OH}^-)/dt = k_L^- \qquad (14)$$

where k_L^- includes wall loss, secondary reactions with species in the OH source, and reaction with O_3 from the ClO reactor. One experimental run consists of a pair of OH-loss measurements to determine k_I^+ and k_I^- under similar conditions. The difference between the two decay rates ($k_I^+ - k_I^-$) and a measurement of the absolute concentration of ClO gives a value for k_1

$$k_1 = (k_I^+ - k_I^-)/[ClO] \qquad (15)$$

This assumes that OH losses due to secondary reactions are small or do not change appreciably when ClO is added: $(k_L^+ - k_L^-) \ll k_1[ClO]$. Evidence that secondary chemistry is unimportant is provided by using two different OH sources and by numerical simulations. These points are discussed below.

Values of k_I^+ and k_I^- are determined from the slopes of ln(I_{OH}) vs l plots by linear least-squares analysis. Typical plots are shown in Figure 2. The reaction length, l, under plug flow conditions determines the reaction time, $t = l/v$, where v is the average flow velocity. Reaction lengths are varied from about 4 to 27 cm, and reaction times range from 2 to 18 ms. Observed first-order rate constants are corrected for axial and radial diffusion by using a method described previously.[19,20] For k_I^+, these corrections range from 3% to 33% and average 15%; for k_I^-, they range from 0.3% to 2% and average 1%. A value of 750 cm^2 s^{-1} is used for the diffusion coefficient of OH in He at 300 K and 1 Torr; a temperature dependence of $T^{1.5}$ is used

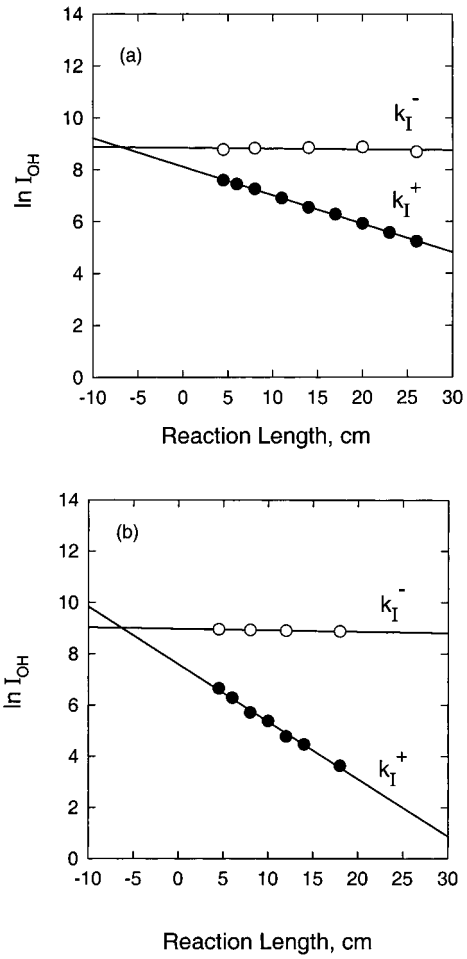

Figure 2. OH decay curves: (○) without added ClO (k_I^-); (●) with added ClO (k_I^+). The lines through the data are linear least-squares fits; panel a conditions were 297.8 K, [ClO] = 8.5×10^{12} cm^{-3}, [O_3] = 1.8×10^{13} cm^{-3}; panel b conditions were 217.5 K, [ClO] = 1.0×10^{13} cm^{-3}, [O_3] = 5.6×10^{13} cm^{-3}.

to estimate the diffusion coefficient at other temperatures.[20] No corrections for viscous pressure drop are made because they are less than 1%.

A summary of experimental conditions and observed rate constants is given in Table 1 and a plot of ($k_I^+ - k_I^-$) vs [ClO] at the two extreme temperatures used in this study is given in Figure 3. The last column of Table 1 gives the values for k_1 obtained from eq 15. Values for k_1 were also obtained from the slopes of the ($k_I^+ - k_I^-$) vs [ClO] plots, and the results are shown in Table 2. Comparison of columns three and four of Table 2 shows that no significant differences are observed between the values obtained from the averages of individual ($k_I^+ - k_I^-$)/[ClO] points and from the slopes of ($k_I^+ - k_I^-$) vs [ClO] plots by linear least-squares fitting. The results reported for the present study are obtained from the averages. An Arrhenius plot of the data is shown in Figure 4 and results in the following expresion:

$$k_1 = (7.2 \pm 2.2) \times 10^{-12} \exp[(+333 \pm 70)/T] \quad (16)$$

for $217.5 \leq T \leq 297.8$ K. The overall measurement error is ±30% obtained from the root-mean-square average of the statistical error (±28%) at the 95% confidence level plus the estimated systematic error (±6%). The statistical error is obtained from an unweighted linear least-squares analysis; the systematic error is discussed below.

TABLE 1: Rate Constant Data for OH + ClO[a]

10^{-12} [ClO], molecule cm^{-3}	10^{-13} [O_3], molecule cm^{-3}	10^{-11} [OH]$_0$, molecule cm^{-3}	[ClO]/[OH]$_0$	($k_I^+ - k_I^-$), s^{-1}	10^{11} k_1, cm^3 molecule^{-1} s^{-1}
$T = 297.8$ K, $P = 1.00$ Torr, $v = 1590$ cm s^{-1}, OH from F + H_2O					
2.82	2.06	2.13	13.2	63.6	2.26
4.05	3.32	3.13	12.9	95.1	2.35
5.85	5.38	5.56	10.5	138.2	2.36
7.17	2.41	3.64	19.7	165.5	2.31
8.21	3.11	5.86	14.0	191.8	2.34
8.46	1.84	3.35	25.2	188.8	2.23
9.27	2.44	3.26	28.4	208.8	2.25
9.32	3.37	6.31	14.8	185.7	1.99
13.4	3.28	6.14	21.8	308.9	2.30
14.5	1.16	3.48	41.7	306.1	2.11
15.6	2.65	5.27	29.6	363.9	2.33
16.1	3.71	5.43	29.6	304.7	1.89
16.6	3.76	5.79	28.7	376.1	2.27
17.0	1.23	3.74	45.4	321.9	1.89
18.4	4.17	5.19	35.4	432.2	2.35
					av = 2.22 ± 0.33
$T = 278.0$ K, $P = 0.986$ Torr, $v = 1489$ cm s^{-1}, OH from F + H_2O					
5.65	2.58	3.69	15.3	131.0	2.32
7.18	3.58	5.11	14.0	166.2	2.31
8.91	1.49	4.94	18.0	194.3	2.18
11.0	1.57	4.72	23.3	251.3	2.28
13.3	2.11	5.37	24.8	322.2	2.42
13.6	0.938	5.43	25.0	322.4	2.37
14.6	3.41	5.98	24.4	398.5	2.73
16.6	4.04	5.24	31.7	414.5	2.50
19.3	1.11	4.52	42.7	509.8	2.64
19.3	3.47	5.16	37.4	506.7	2.62
					av = 2.44 ± 0.36
$T = 259.8$ K, $P = 0.987$ Torr, $v = 1413$ cm s^{-1}, OH from F + H_2O					
3.10	3.72	4.52	6.9	87.1	2.81
3.42	3.17	2.79	12.3	85.6	2.50
3.69	2.83	2.55	14.5	85.5	2.32
6.43	2.41	4.71	13.6	178.0	2.77
9.27	2.64	5.49	16.9	241.8	2.61
12.6	1.16	2.40	52.5	335.5	2.66
13.0	1.12	6.52	19.9	342.8	2.64
13.7	2.67	9.34	14.7	360.3	2.63
14.4	2.28	4.64	31.0	292.3	2.03
17.1	1.88	4.94	34.6	444.5	2.60
19.5	0.603	6.63	29.4	449.3	2.30
					av = 2.53 ± 0.46
$T = 238.6$ K, $P = 1.00$ Torr, $v = 1269$ cm s^{-1}, OH from H + NO_2					
3.45	6.84	4.80	7.2	89.8	2.60
7.57	2.70	3.94	19.2	237.3	3.14
11.1	3.72	4.27	26.0	282.6	2.55
13.5	2.43	4.78	28.2	306.4	2.27
21.5	4.24	4.37	49.2	687.4	3.20
22.5	4.44	4.48	50.2	677.0	3.01
					av = 2.80 ± 0.75
$T = 217.5$ K, $P = 1.02$ Torr, $v = 1132$ cm s^{-1}, OH from H + NO_2					
3.43	6.34	3.20	10.7	119.5	3.48
5.34	6.73	4.98	10.7	200.5	3.76
5.57	5.82	3.65	15.3	196.5	3.53
5.72	5.10	5.73	10.0	215.7	3.77
6.63	6.29	3.48	19.0	215.0	3.24
10.3	5.65	3.84	26.8	291.7	2.83
15.6	5.94	3.99	39.1	633.5	4.06
16.0	5.51	4.56	35.1	548.0	3.42
17.1	5.84	3.26	52.4	485.3	2.84
19.9	5.03	4.34	45.8	664.9	3.34
					av = 3.43 ± 0.78

[a] k_I^+ and k_I^- are corrected for axial and radial diffusion; errors given are two standard deviations.

Discussion

Numerical Modeling and Secondary Chemistry. At the concentrations of OH and ClO and at the [ClO]/[OH]$_0$ ratios used in the present study (see Table 1), secondary reactions are not expected to interfere. To check this, the reaction systems

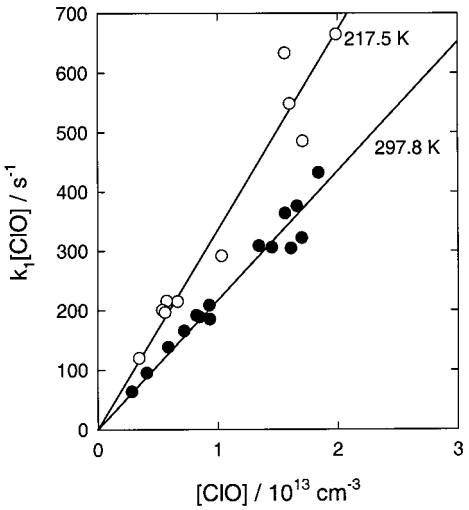

Figure 3. Plot of pseudo-first-order rate constant vs [ClO]. All of the data have been corrected for axial and radial diffusion (see text); lines are linear least-squares fits of the data; temperatures are given next to each plot.

TABLE 2: Summary of Observed Rate Constants for OH + ClO[a]

		10^{11} k_1, cm^3 $molecule^{-1}$ s^{-1}	
T, K	runs	average[b,c]	slope[b,d]
297.8	15	2.22 ± 0.33	2.18 ± 0.24
278.0	10	2.44 ± 0.35	2.52 ± 0.24
259.8	11	2.53 ± 0.46	2.47 ± 0.32
238.6	6	2.80 ± 0.75	2.93 ± 0.64
217.5	10	3.43 ± 0.78	3.36 ± 0.60

[a] Corrected for axial and radial diffusion. [b] Errors are two standard deviations. [c] Average of individual values of k_1. [d] From plots of k_1[ClO] vs [ClO].

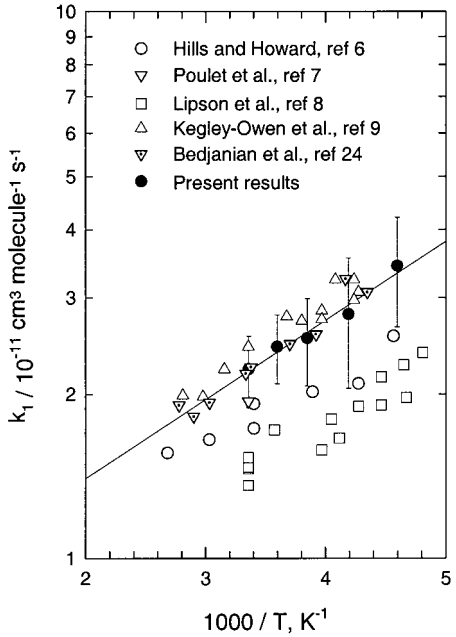

Figure 4. Arrhenius plot of present results compared to earlier studies that also used excess O_3 to produce ClO. The line is the unweighted linear least-squares fit of the present results only; the error bars are two standard deviations.

were simulated by numerical modeling. The procedure and reactions used have been described previously[2] and only an outline is given here. A Gear-based differential equation integrator, CHEMRXN, was used to model each of the ClO and OH sources separately; concentrations, temperatures, pressures, and reaction times were close to those used in actual experimental runs. The results of the source models were then combined to simulate the OH + ClO reaction conditions.

Because there was about a 75 ms transit time between the absorption cell and the start of the OH + ClO reaction, simulations of the ClO source were used to assess the magnitude of ClO loss due mainly to self-reaction (eq 17)

$$ClO + ClO \rightarrow Cl_2 + O_2 \quad (17a)$$

$$ClO + ClO \rightarrow 2Cl + O_2 \quad (17b)$$

$$ClO + ClO \rightarrow OClO + Cl \quad (17c)$$

$$ClO + ClO + He \rightarrow (ClO)_2 + He \quad (17d)$$

In the model, wall loss of ClO was set to zero. Experimental checks for loss of ClO due to wall reaction are discussed below. The modeled ClO concentration at the center of the UV absorption cell, corrected for flow, pressure, and temperature ratios (eq 8), would be the ClO concentration at the start of the OH + ClO reaction if no loss of ClO occurred; it is termed $[ClO]_{uv}$. The loss of ClO is estimated by running the model for 75 ms; the resulting ClO concentration, $[ClO]_{model}$, is then compared to $[ClO]_{uv}$ to assess the magnitude of the loss. From 218 to 298 K, the differences between $[ClO]_{uv}$ and $[ClO]_{model}$ are small: the values range from less than 1% for $[ClO]_{uv} = 3.0 \times 10^{12}$ cm^{-3} to less than 6% for $[ClO]_{uv} = 2.4 \times 10^{13}$ cm^{-3}. Loss of ClO lowers the observed rate constant. However, because the calculated loss is much less than our measurement error of ±30% and because these corrections would act in the opposite direction from those due to secondary chemistry in the OH + ClO reaction system (see below), no corrections were made. Under the conditions used in this study, only small concentrations of the ClO dimer are expected to be produced. The model results show that, even at 218 K, the dimer concentrations are less than 2% of the ClO concentrations at the start of the OH + ClO reaction.

In addition to their effect on ClO concentrations, secondary reactions could contribute to the measured time profile of OH and thereby affect the observed rate constants. Secondary loss of OH would increase the observed rate constants; the most likely interfering reactions of this type are reactions with HO_2 (eq 18), with O_3 (eq 19), and with Cl_2 (eq 20).

$$OH + HO_2 \rightarrow H_2O + O_2 \quad (18)$$

$$OH + O_3 \rightarrow HO_2 + O_2 \quad (19)$$

$$OH + Cl_2 \rightarrow HOCl + Cl \quad (20)$$

Secondary reactions that produce OH could decrease the observed rate constant; the most important reactions in this category are eqs 5b, 21, and 22. HO_2 and Cl are the primary

$$NO + HO_2 \rightarrow OH + NO_2 \quad (21)$$

$$HO_2 + O_3 \rightarrow OH + 2O_2 \quad (22)$$

products of reaction 1, O_3 and Cl_2 are present in the ClO source, and NO is a product of the H + NO_2 reaction (eq 10) used to produce OH in some of the measurements. Because the amount of HO_2 in the system depends on $[OH]_0$, interference from reactions 5b, 18, 21, and 22 is expected to increase as $[OH]_0$

increases. We observe no significant dependence on $[OH]_0$; this may be taken as evidence that these four secondary reactions do not interfere strongly with the measurements. Interference from reaction 19 can be estimated by using $k_{19} = 1.5 \times 10^{-12} \exp(-880/T)$ cm^3 molecule^{-1} s^{-1} [21] and the maximum $[O_3]$ at each temperature. These calculations show that loss of OH by reaction 19 was at most 3% of that by reaction 1 and reaction 19 should not seriously interfere with the rate constant measurements. By using $k_{20} = 1.4 \times 10^{-12} \exp(-900/T)$ cm^3 molecule^{-1} s^{-1},[18] we estimate that loss of OH by reaction 20 is negligible at all temperatures studied.

To more fully check for the effects of secondary chemistry, the OH + ClO reaction system was modeled by combining the model results for the ClO source and the appropriate OH source for the temperature studied. Each experimental run at 218 and 298 K was simulated separately by using ClO, OH, and O_3 concentrations and reaction times that were close to the actual experimental values. Input rate constants, k_1(in), were the experimental values obtained for each run. Wall-loss rate constants for OH, Cl, and ClO were set at 10, 5, and 0 s^{-1}, respectively. The model output consists of [OH] vs reaction time profiles. These were treated in the same way as experimental data to obtain the model value for k_1: plots of ln [OH] vs reaction time were fit by linear regression over time ranges similar to those used in the experiments; the slope gives a value for $-d\ln[OH]/dt$; then from eq 15 and the value for [ClO] in the model, we can obtain k_1(out). At both temperatures, values of k_1(out) are mostly within about ±10% of k_1(in) and the average k_1(out) is 4−6% higher than k_1(in). Because these differences are well within our experimental uncertainty of ±30% and because they tend on average to cancel the effect of ClO loss (see above), no corrections were made. The model results confirm that the major loss of OH in our system is by reaction with ClO with only minor losses from reactions with HO_2 and O_3 (eqs 18 and 19); loss by reaction with Cl_2 (eq 20) is negligible. In addition, the model shows that some minor loss of OH can occur by reaction with the ClO dimer in low-temperature experiments with high initial [ClO]. The simulations show that production rates of OH from reactions 5b, 21, and 22 are small compared to OH loss by reaction with ClO; they also show that in some runs minor amounts of OH can be generated from the reaction of Cl with HOCl (eq 23). HOCl is produced mainly by the reaction of ClO with HO_2 (eq 24) with a small contribution from reaction 20.

$$Cl + HOCl \rightarrow OH + Cl_2 \quad (23)$$

$$ClO + HO_2 \rightarrow HOCl + O_2 \quad (24)$$

Absolute ClO Concentrations. The accuracy of the present measurement depends critically on how well the absolute ClO concentrations are known. ClO concentration is determined by UV absorption as described above and calculated from experimental quantities given by eq 6: A, the absorbance; σ_{ClO}, the absorption cross section; and L, the absorption path length. Uncertainties in each of these are discussed below.

To obtain an experimental value for the absorbance of ClO, an experimental spectrum of ClO plus O_3 is separated by subtracting a scaled ClO reference spectrum.[2,9] The reference spectrum of ClO containing no O_3 (excess Cl atoms) is recorded separately. The scale factor that minimizes the ClO structure in the banded region (265−310 nm) and that also minimizes a calculated residual spectrum is taken as the best value. A separated ClO spectrum is calculated by multiplying the ClO reference spectrum by this scale factor; then the absorbance of

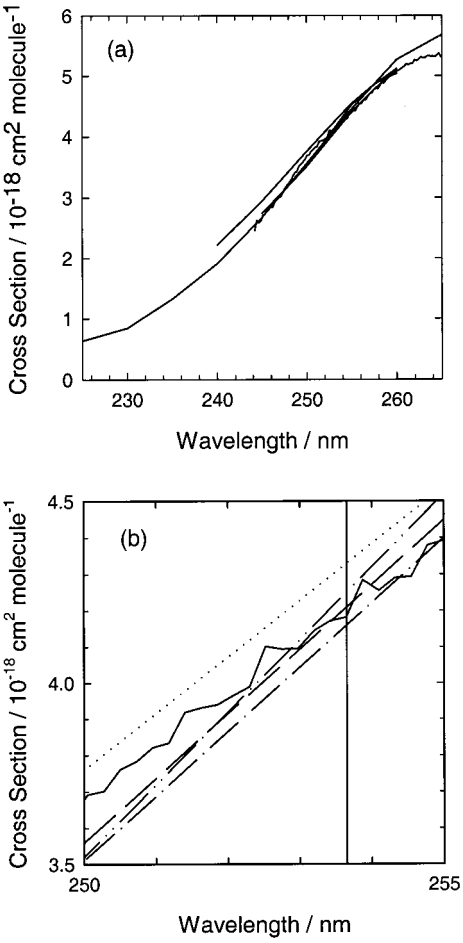

Figure 5. (a) Absorption cross sections of ClO in the continuum region from 225 to 265 nm; (b) expanded view of the region from 250 to 255 nm. References are Johnston et al.[13] (dashed line), Mandelman & Nicholls[14] (dashed−dot−dot line), Sander & Friedl[15] (dashed−dot line), Simon et al.[16] (dotted line), Bloss[17] (solid line). Vertical line is at 253.65 nm.

ClO is determined at 253.65 nm in the continuum of the separated spectrum where the cross sections are independent of temperature.[22] The residual spectrum is calculated by subtracting the separated ClO and O_3 spectra from the original combined spectrum. The residual absorbance at all wavelengths is less than 0.1% of the absorbance of the separated spectra; this shows that O_3 makes no significant contribution to the separated ClO absorbance that is used to obtain [ClO]. We can estimate the precision of the method by repeating the same subtraction several times; the resulting [ClO] varies about ±4%.

There have been several measurements of the ClO absorption cross section in the continuum region.[13−17] Figure 5 is summary plot of these studies. The results using different measurement techniques are all in very good agreement and yield an average value of $(4.23 \pm 0.13) \times 10^{-18}$ cm^2 molecule^{-1} at 253.65 nm; the errors given are twice the standard deviation of the average. From this, we estimate an uncertainty of about 3−4% in the value of σ_{ClO}.

The accuracy in determining the absorption path length, L, is about ±1%. Combining this with the uncertainties in the absorbance and cross section gives an estimated uncertainty of ±6% in the ClO concentration measurements in the UV absorption cell.

Loss of ClO can occur between the absorption cell and the start of the OH + ClO reaction; ClO can also be lost over the

measurement time of the OH decay. Between the cell and the point where the reaction starts, this loss is due mainly to self-reaction (eq 17) and to reaction at the wall. As discussed above, numerical models of the ClO source show that the losses due to self-reaction are less than 6%. Models also show that at the stoichiometric ratios used in the present experiments, loss of ClO during the measurement time is small (generally about 2−5%). Experimental tests described below show that ClO wall loss is small in our system. Combining the uncertainties in the absorbance (±4%), cross section (±4%), path length (±1%), and reaction losses (about ±10%), we estimate the uncertainty in the absolute ClO concentration measurements to be about ±12%.

ClO Wall Loss. In low surface to volume reactors, wall loss of ClO generally ranges from less than 0.1 to 2 s^{-1} even at very low temperatures.[7,18,23] In our system, the surface to volume ratio changes by about 45% when the OH source is moved along the main reactor axis; this can serve as a rough experimental check for large ClO wall losses. If significant ClO wall losses occurred, the [ClO] would strongly depend on the position of the OH source (the reaction length) and nonlinear $\ln(I_{OH})$ vs l plots should result. All of the OH decay plots were linear, and this is consistent with no major loss of ClO on the main reactor surfaces. To further check for ClO wall loss between the absorption cell and the main reactor, we converted ClO to Cl atoms by adding an excess of NO (eq 25) in the main reactor 75 ms after ClO was determined by UV absorption.

$$ClO + NO \rightarrow Cl + NO_2 \qquad (25)$$

This is close to the timing in the actual rate measurements. Assuming one-to-one stoichiometry for the ClO to Cl conversion from reaction 25, [ClO] inferred from [Cl] agrees with [ClO] calculated from the UV absorption measurements within about 15%. The overall accuracy of these measurements is estimated at ±20%, mainly because of uncertainties in the Cl lamp calibrations. The results show that there is no large wall loss of ClO between the absorption cell and the start of the OH + ClO reaction. No correction for wall loss is made because these experiments cannot determine it precisely and the estimate is well within the experimental uncertainty.

Error Analysis. An estimate of systematic and overall experimental errors in determining k_1 can be made by considering that under plug flow conditions eqs 13 and 14 become

$$k_I^+ \equiv -v\{d\ln(I_{OH}^+)/dl\} = k_1[ClO] + k_L^+ \qquad (26)$$

$$k_I^- \equiv -v\{d\ln(I_{OH}^-)/dl\} = k_L^- \qquad (27)$$

In a cylindrical reactor, the average flow velocity, v, is given by

$$v = (760/P)(T/273.2)(F/(60\pi a^2)) \qquad (28)$$

where P is the flow pressure in Torr, T is the absolute temperature, F is the mass flow in standard $cm^3\ min^{-1}$, and a is the reactor radius in cm. From eqs 6, 15, 26, and 27, we have

$$k_1 = -v\{d\ln(I_{OH}^+)/dl - d\ln(I_{OH}^-)/dl\}(\sigma_{ClO}L/A) \qquad (29)$$

Systematic errors in k_1 include errors in v, σ_{ClO}, and L; errors in $\{d\ln(I_{OH}^+)/dl - d\ln(I_{OH}^-)/dl\}$ and A are measurement or statistical errors. The errors in v comprise errors in P, T, F, and a, which we estimate at ±2%, ±1%, ±4%, and ±2%, respectively. We have discussed above the error estimates for σ_{ClO} (±4%) and L (±1%). Taking the root-mean-square average of the systematic errors, we estimate the overall systematic error at ±6%. Combining the systematic error with the measurement (statistical) error of ±28% in k_1, we estimate an overall uncertainty of ±30% in k_1 at the 95% confidence level.

Comparison with Other Studies. A summary of rate constant measurements for the OH + ClO reaction is presented in Table 3. The first three entries[3−5] in the table used excess Cl atoms to produce ClO from reactions 2, 3, or 4 and assumed that [ClO] was equal to initial [O_3], [Cl_2O], or [OClO]. Subsequent studies have shown that this assumption is not always true; for the measurement to be useful, experimental checks are needed to verify the assumption.[7,9,10] Use of excess Cl atoms also creates a secondary source of OH from reaction 5b and necessitates a correction procedure. These complications probably account for the relatively low results reported by these early studies, and they are not considered further in this discussion. The next five entries[6−9,24] plus the present study used excess O_3 to produce ClO; the studies by Poulet et al.[7] and Bedjanian et al.[24] used both excess Cl atoms and excess O_3 (or OClO). Except for the study by Lipson et al.,[8] the agreement among these studies is reasonably good: k_1 at 298 K ranges from 1.8×10^{-11} to 2.4×10^{-11} cm^3 $molecule^{-1}$ s^{-1} with an average value of 2.1×10^{-11} cm^3 $molecule^{-1}$ s^{-1}; the Arrhenius parameters are also in good agreement over the temperature ranges studied.

Because all of the studies used ClO in excess, differences in the results may be due to the methodology and accuracy of the various techniques used to determine absolute ClO concentrations. Hills and Howard[6] measured k_1 with a slight excess of O_3 over Cl atoms but calibrated their ClO detection sensitivity by using reaction 2 with excess Cl atoms and assumed [ClO] = $[O_3]_0$. However, they checked this assumption by titrating the ClO with NO (eq 25), and the titration agreed with the calibration results within 10%.

Poulet et al.[7] used both excess Cl atoms and excess O_3 to measure k_1. In both cases, they determined absolute [ClO] by the NO titration method and obtained similar results (see Table 3).

Lipson et al.[8] detected ClO by using chemi-ionization mass spectrometry following a charge-transfer reaction (eq 30). ClO

$$ClO + SF_6^- \rightarrow ClO^- + SF_6 \qquad (30)$$

was calibrated as NO_2 by adding an excess of NO (eq 25). Because excess O_3 was used, they added C_2H_6 to scavenge (eq 31) the Cl atoms produced by reaction 25 to prevent reformation

$$Cl + C_2H_6 \rightarrow HCl + C_2H_5 \qquad (31)$$

of ClO from Cl + O_3 (eq 2). They modeled this system to correct for the small amount of NO_2 lost by reaction with C_2H_5; these corrections were less than 15%. Their result at 298 K is about 40% lower than the average of the five other measurements using excess O_3. Although they do not explicitly discuss NO_2 formation from the reaction of NO with excess O_3 (eq 32), we have tried to estimate the amount of added NO_2 formed

$$NO + O_3 \rightarrow NO_2 + O_2 \qquad (32)$$

by reaction 32 in their system and find that it should be less than 2% of the NO_2 formed from ClO + NO (eq 25) and thus cannot explain the difference in our results. They also did not correct their results for the effects of turbulent flow, which they estimate lowered their k_1 measurement by about 8%. Making

TABLE 3: Summary of OH + ClO Rate Constant Measurements

10^{12} k_1,[a] cm^3 molecule^{-1} s^{-1}	T, K	P, Torr	method[b]	comments[c]	ref
9.1 ± 2.6	298	1.0−3.5 He	DLF−RF	ClO from O_3 (Cl_2O) + excess Cl; OH from H + NO_2	Leu, 1979[3]
11.7 ± 3.3 independent of T	248−335	1 He	DLF−RF	ClO from O_3 + excess Cl; correct for Cl + HO_2; OH from H + NO_2	Ravishankara et al., 1983[4]
11.9 ± 1.8 independent of T	243−298	1−5 He	DLF−RF	ClO from O_3 + excess Cl; correct for Cl + HO_2; OH from H + NO_2	Burrows et al., 1984[5]
(8.0 ± 1.4) exp[(235 ± 46)/T]; 17.5 ± 3.1 at 298 K	219−373	1.0−1.1 He	DLF-LMR	ClO from Cl + excess O_3; OH from H + NO_2	Hills and Howard, 1984[6]
19.9 ± 2.5 (excess Cl), 18.9 ± 2.1 (excess O_3), 19.4 ± 3.8 (all data)	298	0.5−0.9 He	DLF-LIF (OH), EIMS (ClO)	ClO from Cl + O_3 (ClO_2); ClO determined as NO_2 after NO + ClO; use both excess O_3 (ClO_2) and excess Cl; correct for Cl + HO_2; OH from H + NO_2	Poulet et al., 1986[7]
(5.5 ± 1.6) exp[(292 ± 72)/T]; 14.6 ± 2.3 at 298 K	205−298	100 N_2	DTF−CIMS	ClO from Cl + excess O_3; ClO determined as NO_2 after ClO + NO; OH from H + NO_2	Lipson et al., 1997[8]
(8.9 ± 2.7) exp[(295 ± 95)/T]; 24.4 ± 0.7 at 298 K	234−356	4.2−15.4 He	DLF−UVA (ClO), FP-LIF (OH)	ClO from Cl + excess O_3; ClO by UV absorption; OH from photolyis of O_3 + H_2O or HNO_3	Kegley-Owen et al., 1999[9]
(6.7 ± 1.8) exp[(360 ± 90)/T]; 22 ± 4 at 298 K	230−360	1.0 He	DLF-EIMS	ClO from Cl + O_3; ClO determined as NO_2 after ClO + NO; use both excess O_3 and excess Cl; OH from H + NO_2	Bedjanian et al., 2001[24]
(7.2 ± 2.2) exp[(333 ± 70)/T]; 22.2 ± 3.3 at 298 K	218−298	1.0 He	DLF−RF−UVA	ClO from Cl + excess O_3; ClO by UV absorption; OH from F + H_2O and H + NO_2	present study

[a] Uncertainties are two standard deviations. [b] CIMS = chemical ionization mass spectrometry; DLF = discharge laminar flow; DTF = discharge turbulent flow; EIMS = electron impact mass spectrometry; FP = flash photolysis; LIF = laser induced fluorescence; LMR = laser magnetic resonance; RF = resonance fluorescence; UVA = ultraviolet absorption spectrometry. [c] Pseudo-first-order in OH ([ClO] ≫ [OH]).

this correction would improve agreement, but their result would still be lower than the other excess O_3 measurements by about 30%. The reason for this discrepancy remains unclear at this time.

Our results agree very well with the recent measurements of Kegley-Owen et al. (KO).[9] Although both studies used UV absorption to monitor ClO, the measurements differ in some of the detailed parameters needed to determine absolute concentrations of ClO. KO measured ClO in the actual reactor tube where the OH + ClO reaction occurred. In their experiments, the absorption path length could not be measured directly because of uncertainties as to how well the flow dynamics confined the ClO radicals in the UV absorption path and the possible presence of stagnation regions. The absorption path length was calibrated by comparing the optical density of O_3 measured in a cell of known path length in series with the OH + ClO reactor with the O_3 optical density in the reactor. In the present study, ClO was measured in an absorption cell of known path length upstream of the main OH + ClO reactor and absolute ClO concentrations were obtained by adjusting for mass flow, pressure, and temperature differences between the absorption cell and the main reactor (eq 8). The two studies differ also in the methods used to generate OH radicals. KO used flash photolysis of O_3 plus H_2O mixtures or of HNO_3; the present study used F + H_2O (eq 9) and H + NO_2 (eq 10) as described above.

Our results also agree very well with a recent measurement by Bedjanian et al.[24] In this study, mass spectrometry was used to detect ClO as NO_2 following the NO + ClO reaction (eq 25). The mass spectrometer signal was calibrated by using an excess of Cl atoms to generate a known amount of ClO from Cl + O_3 (eq 2). This calibration was checked under excess O_3 conditions by measuring the fraction of Cl_2 dissociated to form Cl atoms. The two methods agreed within a few percent. The rate constant was measured under pseudo-first-order conditions ([ClO] ≫ $[OH]_0$) by using both excess O_3 and excess Cl atoms to produce ClO. Numerical simulations were used to correct the observed decay rates for secondary chemistry. Under excess O_3, the main interference was OH + HO_2 (eq 18); under excess Cl atoms, the main interference was Cl + HO_2 (eq 5b). After making the corrections, the results obtained under the two reaction conditions agree very well.

The excellent agreement among the latest three studies, which used a variety of OH sources and entirely different detailed experimental methods to determine absolute [ClO], is good evidence that secondary chemistry did not interfere and that [ClO] was accurately measured.

Acknowledgment. The research described in this article was performed at the Jet Propulsion Laboratory, California Institute of Technology, under a contract with the National Aeronautics and Space Administration. We thank William Bloss for communicating his results on ClO absorption cross sections and Yuri Bedjanian for sending his results on the OH + ClO reaction.

References and Notes

(1) Chance, K.; Traub, W. A.; Johnson, D. G.; Jucks, K. W.; Ciarpallini, P.; Stachnik, R. A.; Salawitch, R. J.; Michelsen, H. A. *J. Geophys. Res.* **1996**, *101*, 9031.

(2) Wang, J. J.; Keyser, L. F. *J. Phys. Chem. A* **2001**, *105*, 6479.

(3) Leu, M. T.; Lin, C. L. *Geophys. Res. Lett.* **1979**, *6*, 425.

(4) Ravishankara, A. R.; Eisele, F. L.; Wine, P. H. *J. Chem. Phys.* **1983**, *78*, 1140.

(5) Burrows, J. P.; Wallington, T. J.; Wayne, R. P. *J. Chem. Soc., Faraday Trans. 2* **1984**, *80*, 957.

(6) Hills, A. J.; Howard, C. J. *J. Chem. Phys.* **1984**, *81*, 4458.

(7) Poulet, G.; Laverdet, G.; Le Bras, G. *J. Phys. Chem.* **1986**, *90*, 159.

(8) Lipson, J. B.; Elrod, M. J.; Beiderhase, T. W.; Molina, L. T.; Molina, M. J. *J. Chem. Soc., Faraday Trans.* **1997**, *93*, 2665.

(9) Kegley-Owen, C. S.; Gilles, M. K.; Burkholder, J. B.; Ravishankara, A. R. *J. Phys. Chem. A* **1999**, *103*, 5040.

(10) Burkholder, J. B.; Hammer, P. D.; Howard, C. J.; Goldman, A. *J. Geophys. Res.* **1989**, *94*, 2225.

(11) Wang, J. J.; Keyser, L. F. *J. Phys. Chem. A* **1999**, *103*, 7460.

(12) Molina, L. T.; Molina, M. J. *J. Geophys. Res.* **1986**, *91*, 14501.

(13) Johnston, H. S.; Morris, E. D., Jr.; Van den Bogaerde, J. *J. Am. Chem. Soc.* **1969**, *91*, 7712.

(14) Mandelman, M.; Nicholls, R. W. *J. Quant. Spectrosc. Radiat. Transfer* **1977**, *17*, 483.

(15) Sander, S. P.; Friedl, R. R. *J. Phys. Chem.* **1989**, *93*, 4764.

(16) Simon, F. G.; Schneider, W.; Moortgat, G. K.; Burrows, J. P. *J. Photochem. Photobiol. A: Chem.* **1990**, *55*, 1.

(17) Bloss, W. J., Ph.D. Thesis, University of Cambridge, 1999.

(18) DeMore, W. B.; Sander, S. P.; Howard, C. J.; Ravishankara, A. R.; Golden, D. M.; Kolb, C. E.; Hampson, R. F.; Kurylo, M. J.; Molina, M. J. *Chemical Kinetics and Photochemical Data for Use in Stratospheric Modeling, Evaluation No. 12*; JPL Publication 97-4; Jet Propulsion Laboratory, California Institute of Technology: Pasadena, CA, 1997.

(19) Brown, R. L. *J. Res. Natl. Bur. Stand. (U. S.)* **1978**, *83*, 1.

(20) Keyser, L. F. *J. Phys. Chem.* **1984**, *88*, 4750.

(21) Sander, S. P.; Friedl, R. R.; DeMore, W. B.; Ravishankara, A. R.; Golden, D. M.; Kolb, C. E.; Kurylo, M. J.; Hampson, R. F.; Huie, R. E.; Molina, M. J.; Moortgat, G. K. *Chemical Kinetics and Photochemical Data for Use in Stratospheric Modeling, Evaluation No. 13*; JPL Publication 00-3; Jet Propulsion Laboratory, California Institute of Technology: Pasadena, CA, 2000.

(22) Trolier, M.; Mauldin, R. L., III; Ravishankara, A. R. *J. Phys. Chem.* **1990**, *94*, 4896.

(23) Lee, Y.-P.; Stimpfle, R. M.; Perry, R. A.; Mucha, J. A.; Evenson, K. M.; Jennings, D. A.; Howard, C. J. *Int. J. Chem. Kinet.* **1982**, *14*, 711.

(24) Bedjanian, Y.; Riffault, V.; Le Bras, G. *Int. J. Chem. Kinet.*, in press. We became aware of these measurements after we submitted the present study for publication.